

This discussion paper is/has been under review for the journal Hydrology and Earth System Sciences (HESS). Please refer to the corresponding final paper in HESS if available.

Stem-root flow effect on soil–atmosphere interactions and uncertainty assessments

T.-H. Kuo¹, J.-P. Chen¹, and Y. Xue²

¹Department of Atmospheric Sciences, National Taiwan University, Taipei, Taiwan, Republic of China

²Department of Atmospheric and Oceanic Sciences, and Department of Geography, University of California, Los Angeles, California, USA

Received: 1 October 2015 – Accepted: 27 October 2015 – Published: 11 November 2015

Correspondence to: J.-P. Chen (jpchen@as.ntu.edu.tw)

Published by Copernicus Publications on behalf of the European Geosciences Union.

HESSD

12, 11783–11816, 2015

Stem-root flow effect on soil–atmosphere interactions and uncertainty assessments

T.-H. Kuo et al.

Title Page

Abstract

Introduction

Conclusions

References

Tables

Figures

⏪

⏩

◀

▶

Back

Close

Full Screen / Esc

Printer-friendly Version

Interactive Discussion

Abstract

Soil water can rapidly enter deeper layers via vertical redistribution of soil water through the stem–root flow mechanism. This study develops the stem–root flow parameterization scheme and coupled this scheme with the Simplified Simple Biosphere model (SSiB) to analyze its effects on land–atmospheric interactions. The SSiB model was tested in a single column mode using the Lien Hua Chih (LHC) measurements conducted in Taiwan and HAPEX-Mobilhy (HAPEX) measurements in France. The results show that stem–root flow generally caused a decrease in the moisture content at the top soil layer and moistened the deeper soil layers. Such soil moisture redistribution results in significant changes in heat flux exchange between land and atmosphere. In the humid environment at LHC, the stem–root flow effect on transpiration was minimal, and the main influence on energy flux was through reduced soil evaporation that led to higher soil temperature and greater sensible heat flux. In the Mediterranean environment of HAPEX, the stem–root flow significantly affected plant transpiration and soil evaporation, as well as associated changes in canopy and soil temperatures. However, the effect on transpiration could either be positive or negative depending on the relative changes in the moisture content of the top soil vs. deeper soil layers due to stem–root flow and soil moisture diffusion processes.

1 Introduction

The water stored in the land system is a key factor controlling many physical processes and feedback between the land and atmosphere. Soil moisture is a source of water for the atmosphere through processes that lead to evapotranspiration, including bare soil evaporation, plant transpiration and evaporation from other surfaces such as leaves, snow, etc. The rainfall redistribution process in forest systems affects soil water amount and its distribution (McGuffie et al., 1995; Chase et al., 1996, 2000; Zhao et al., 2001). Rain water entering the forest is redistributed via several pathways before

Stem-root flow effect on soil–atmosphere interactions and uncertainty assessments

T.-H. Kuo et al.

[Title Page](#)

[Abstract](#)

[Introduction](#)

[Conclusions](#)

[References](#)

[Tables](#)

[Figures](#)



[Back](#)

[Close](#)

[Full Screen / Esc](#)

[Printer-friendly Version](#)

[Interactive Discussion](#)



Stem-root flow effect on soil–atmosphere interactions and uncertainty assessments

T.-H. Kuo et al.

[Title Page](#)

[Abstract](#)

[Introduction](#)

[Conclusions](#)

[References](#)

[Tables](#)

[Figures](#)

[⏪](#)

[⏩](#)

[◀](#)

[▶](#)

[Back](#)

[Close](#)

[Full Screen / Esc](#)

[Printer-friendly Version](#)

[Interactive Discussion](#)



reaching the forest floor, e.g., some is intercepted by the canopy and some reaches the soil as throughfall. A significant amount of rainwater intercepted by the canopy can flow down along tree stems and reach the forest floor in a process termed stemflow. The efficiency of stemflow varies with plant species, seasons, meteorological conditions, rainfall intensity, and canopy structure (Levia and Frost, 2003). Johnson and Lehmann (2006) summarized various field measurements and showed that the fraction of precipitation that becomes stemflow ranges from 0.07 to 22 %.

In contrast to the throughfall that infiltrates slowly through the top soil, stemflow can continue via the root system (hereafter called the “stem–root flow”) and quickly reach deep soil layers and the water table (Liang et al., 2007). It has long been recognized that the stem–root flow can help to store water in deeper soil layers and thus create favorable conditions for plant growth under arid conditions (Návar, 1993; Li et al., 2009). Soil water redistribution by stem–root flow not only affects vegetation growth but also land evapotranspiration and runoff (Neave and Abrahams, 2002). Furthermore, the enhanced water penetration can significantly alter groundwater recharge. Taniguchi et al. (1996) showed that in a pine forest, the stem–root flow contributed approximately 10–20 % of annual groundwater recharge even with a stemflow-to-precipitation ratio of only 1 %.

Stem–root flow effects have not been considered in most land–surface schemes of climate models. Tanaka et al. (1996) developed a model to evaluate the effect of stem–root flow on groundwater. This model is yet to be implemented in current land surface models. Li et al. (2012) pointed out that stemflow hydrology and preferential flow along roots are intimately linked, but direct integration of these processes into land models, to our knowledge, has not been reported.

In this paper, we parameterized the stem–root flow processes in a land surface model named the Simplified Simple Biosphere Model (SSiB; Xue et al., 1991), and analyzed how stem–root flow affects soil moisture and whether this effect is significant enough to influence atmospheric processes. Soil moisture data from two sites, located at Lien Hua Chih, Taiwan (LHC) and Bordeaux/Toulouse, France (from the HAPEX-Mobilhy

experiment, hereafter called HAPEX), were collected for model evaluation. The two sites represent different climate regimes and terrestrial ecosystem, and stem–root flow modifies their surface energy and water processes in somewhat dissimilar ways.

2 Methodology

2.1 The stem–root flow model

In the original SSiB land surface model (Xue et al., 1996), vertical soil water movement is described by the diffusion equations:

$$\begin{aligned} \frac{\partial \theta_1}{\partial t} &= \frac{1}{D_1} [P + Q_{12} - E_{SE} - b_1 E_{TR,1}] \\ \frac{\partial \theta_2}{\partial t} &= \frac{1}{D_2} [-Q_{12} + Q_{23} - b_2 E_{TR,2}] \\ \frac{\partial \theta_3}{\partial t} &= \frac{1}{D_3} [-Q_{23} + Q_3 - b_3 E_{TR,3}] \end{aligned} \quad (1)$$

where the subscripts 1, 2 and 3 are indices of the top, middle, and bottom soil layers, respectively; θ is the soil water content, expressed as a fraction of the saturated value; D is soil thickness; P is effective precipitation flux on the soil surface, composed of the direct throughfall and the throughfall from leave-intercepted rainfall (cf. Fig. 1); $Q_{ij} = -k [\partial \Psi / \partial z + 1]$ is the flux of water between the i th and j th layers, and is defined to be positive in an upward direction; Ψ (in m) is the soil water potential; E_{SE} is the evaporation rate of bare soil; i is the soil layer index; $E_{TR,i}$ is the transpiration rate in soil layer; b_i is the proportionality factor that accounts for root distribution; Q_3 is the water flux entering the water table. The similar approach has been used by many land surface models. Note that the middle soil layer can be divided into more sublayers with similar formula as used for the middle layer. In these equations, the transfer velocity Q_{ij}

considers only the soil diffusion flow. This study develops the parameterizations that include the stem–root flow mechanism which provides a “bypass” for water to channel through the soil on root surfaces (Fig. 1). The stemflow reaching the top soil layer, q_0 , is often represented as a fraction of the total precipitation (or, more precisely, the leaf drainage) such that direct rainfall entering the soil becomes

$$P' \equiv P - q_0. \quad (2)$$

After entering the soil, the root flow is divided into a downward transfer flux q_z (within the root system) and a lateral transfer flux q_x (from the root surface to the soil). These two fluxes can be parameterized as following:

$$q_{z,i} = \alpha_z A_i h_i V_s \quad (3)$$

$$q_{x,i} = \begin{cases} \alpha_x R_i A_i K (\Psi_i) \left(\frac{\Psi_i - \Psi_s}{D_{\text{eff}}} \right), & \text{if } h_i > 0 \\ 0, & \text{if } h_i = 0 \end{cases} \quad (4)$$

where α_z and α_x are proportionality coefficients; A_i (in $\text{m}^2 \text{m}^{-3}$) is the total root surface area density that varies with vegetation types (Böhm, 1979; Zhang et al., 2005; Li et al., 2013); h_i (in m) is the thickness of water on the root surface; V_s (in m s^{-1}) is the terminal velocity of root flow; R_i (in m) is the root length; K (in m s^{-1}) is the hydraulic conductivity of the soil; Ψ_s (in m) is the soil water potential at saturation; Ψ_i (in m) is the soil water potential; and D_{eff} (in m) is the effective thickness of the water–soil interface. Derivation

Stem-root flow effect on soil–atmosphere interactions and uncertainty assessments

T.-H. Kuo et al.

Title Page

Abstract

Introduction

Conclusions

References

Tables

Figures

◀

▶

◀

▶

Back

Close

Full Screen / Esc

Printer-friendly Version

Interactive Discussion



of D_{eff} is described in the Appendix. From Eqs. (1), (2) and (4), we have:

$$\begin{aligned}\frac{\partial \theta_1}{\partial t} &= \frac{1}{D_1} [P' + Q_{12} - E_{\text{SE}} - b_1 E_{\text{TR},1} + q_{x,1}] \\ \frac{\partial \theta_2}{\partial t} &= \frac{1}{D_2} [-Q_{12} + Q_{23} - b_2 E_{\text{TR},2} + q_{x,2}] \\ \frac{\partial \theta_3}{\partial t} &= \frac{1}{D_3} [-Q_{23} + Q_3 - b_3 E_{\text{TR},3} + q_{x,3}]\end{aligned}\quad (5)$$

5 In Eq. (3), the root surface water thickness h_i is determined by the input root flow amount (q_0), total root surface area in the soil layer, and horizontal root flow. Its tendency can be described as:

$$\frac{dh_i}{dt} = \begin{cases} \frac{(q_{z,i-1} - q_{z,i} - q_{x,i})}{A_i R_i} & , \text{ if } h_i > 0 \\ 0 & , \text{ if } h_i = 0 \end{cases}\quad (6)$$

10 Equations (5) and (6) represent the water budgets in the soil and root flow systems, respectively, and they are linked through the term q_x in Eq. (4).

Stemflow input into the first soil layer (q_0) is represented as a fraction of the leaf drainage (LD), which is the portion of precipitation that is intercepted by the canopy minus leaf evaporation and can be calculated in SSiB. LD is similar to canopy drip in some other models, and is represented mainly as a function of the leaf area index (LAI). The ratio of q_0 to LD depends mainly on plant type, as well as meteorological conditions such as wind speed (Levia and Frost, 2003; Johnson and Lehmann, 2006; André et al., 2008; Siegert and Levia, 2014). Unfortunately, there is still insufficient information to determine the ratio of q_0 to LD. We conducted a series of sensitivity tests with systematically varying ratio between the q_0 and LD to assess the uncertainty.

20 The stem–root flow parameterization was tested using the offline SSiB, which is a simplified version of the land-biosphere model developed by Sellers et al. (1986). The model recognizes 12 different vegetation types according to Dorman and Sellers

(1989), and is set up with 3 soil layers and 1 canopy layer. The SSiB model has 8 prognostic variables: soil wetness for 3 layers; temperature at the canopy, ground surface and deep soil layers; snow depth at ground level; and water intercepted by the canopy. An additional variable – h_i – was added for each soil layer to account for the stem–root flow mechanism. An implicit backward scheme was used to calculate the temperature tendency in the coupling of the lowest atmospheric model layer with SSiB, such that energy conservation between the land surface and the atmosphere was satisfied. Soil temperature was calculated using the force-restore method, and water movement in the soil was described by the diffusion equation as shown in Eq. (5).

2.2 Experimental design and site information

Two sites with different climate and vegetation conditions were selected to test the stem–root flow parameterizations in the SSiB model. The first is a site with warm-to-temperate mountain rainforest condition from the Lien Hua Chi (LHC; 23°55′ N, 120°53′ E), Taiwan. LHC is located in the Central Mountain Range of Taiwan, with a hilly terrain and a mean altitude of 770 m a.s.l. in the surroundings. The average annual rainfall at LHC is 2317 mm, with rain falling predominantly in late summer and early autumn (Fig. 2). With ample rainfall, LHC is covered with dense forest with an average canopy height of approximately 17 m. The vegetation cover is comprised of mixed evergreens and hardwood species, including *Cryptocarya chinensis*, *Engelhardtia roxburghiana*, *Tutcheria shinkoensis*, and *Helicia formosana*. The soil has a loamy texture with an average bulk density of 1.29 g cm⁻³ and a porosity of 0.53 over the top 1.0 m (Chen, 2012). Soil moisture measurements were collected at depths of 10, 30, 50, 70 and 90 cm, and hourly precipitation was measured on site.

The second is the HAPEX-Mobilhy data collected at the Caumont site (SAMER station No. 3; 43°41′ N, 0°6′ W) with an elevation of 113 m a.s.l. and relatively flat terrain. This site has a Mediterranean climate, with an annual rainfall of 856 mm, most of which occurs in spring and winter (Fig. 3). In contrast to the LHC site with dense forest, the HAPEX site is covered mostly with short and sparse soya crops, and the surface

Stem-root flow effect on soil–atmosphere interactions and uncertainty assessments

T.-H. Kuo et al.

Title Page

Abstract

Introduction

Conclusions

References

Tables

Figures

⏪

⏩

◀

▶

Back

Close

Full Screen / Esc

Printer-friendly Version

Interactive Discussion



conductivity, which was measured as $4 \times 10^{-6} \text{ ms}^{-1}$ at HAPEX and $1 \times 10^{-6} \text{ ms}^{-1}$ at LHC. Therefore, we set the root-flow velocity V_s as 10^{-4} ms^{-1} in the simulation, and will discuss the associated uncertainty later.

The SLR value depends on a number of parameters as discussed in the previous section. This study evaluated SLR-introduced uncertainty by conducting sensitivity tests with systematically varying SLR from 0 to 100%, and identified optimal value that yielded the best soil moisture profiles compared with the observations. The optimal SLR value for the HAPEX experiment was approximately 50%, compared with 90% for the LHC case. These values reflect the large contrast in leaf coverage and plant type between the two sites. In these experiments, we set A_i to $0.5 \text{ m}^2 \text{ m}^{-3}$ based on the Li et al. (2013) and the proportionality coefficients, α_z and α_x , are set to 1. The uncertainty discussion for V_s and SLR should include the uncertainty caused by these parameters. When more observational data are available, we could revisit these issues further. All simulations used integration time step of 30 min.

3 Effect of stem–root flow on soil moisture

The modified SSiB model was used to simulate the intra-annual variations in soil conditions for the 2010 LHC case and the 1986 HAPEX case. For the LHC case, the simulation well captured the soil moisture increase associated with precipitation events followed by rapid drying (Fig. 4). In many instances, the simulated soil moisture fluctuation was stronger in the middle layer than in the top or bottom layers, as found in the observations. The shading shows the range of uncertainty due to different SLRs (from 0 to 100%). When SLR is zero, which has no stem flow effect and is referred to as the control run in this paper, the soil moisture of the middle layer is very low and fluctuates less in response to rainfall events (Fig. 4). The simulation generally underestimated the soil moisture in the bottom layer even with the root-flow mechanism. In the top layer, the model overestimated soil moisture in spring and winter, but underestimated it during autumn. Such discrepancies are generally less substantial when the stem–root flow

Stem-root flow effect on soil–atmosphere interactions and uncertainty assessments

T.-H. Kuo et al.

Title Page

Abstract

Introduction

Conclusions

References

Tables

Figures

⏪

⏩

◀

▶

Back

Close

Full Screen / Esc

Printer-friendly Version

Interactive Discussion



mechanism is included, as indicated by the generally lower bias and root-mean-square error shown in Table 3. The possible causes of error will be elaborated in the discussion section.

For the HAPEX case, the simulations also well captured the seasonal cycle as well as the sharp fluctuations in the top layer (Fig. 5). Without the stem–root flow mechanism, soil moisture was generally overestimated in the two upper layers and underestimated in the bottom layer, except during April and May when all layers were too dry. When stem–root flow with SLR = 50 % was considered, the model performed better in all layers (see Table 3). Stem–root flow with a much higher SLR (e.g., SLR = 100 %) produced worse results for soil moisture in the surface and middle layers. Note that SLR = 50 % produced the driest middle layer, indicating that the stem–root flow effect is nonlinear because both stem–root flow and diffusion, as well as their interactions, play role in soil moisture variations. In the bottom layer, more accurate soil moisture was obtained with SLR = 100 %, but this does not necessarily mean that the stem–root flow was underestimated. We suspect that the discrepancy in the bottom layer was caused mainly by the excess drainage of soil water from the lower boundary in the model and will elaborate this issue in the discussion section.

It is also worth mentioning that both the observation and simulation showed weaker soil moisture fluctuations in the middle than in the surface layer, a feature very different from the LHC case. It is likely that there is a weaker stem–root flow associated with plant and soil types in the HAPEX case. Figures 4 and 5 demonstrate that the strength of the stem–root flow is greater in LHC, with associated changes in soil moisture of up to $0.1 \text{ m}^3 \text{ m}^{-3}$ compared with the maximum changes of $0.05 \text{ m}^3 \text{ m}^{-3}$ at HAPEX. This stronger stem–root flow effect was mainly associated with the more intense rainfall at LHC.

HESSD

12, 11783–11816, 2015

Stem-root flow effect on soil–atmosphere interactions and uncertainty assessments

T.-H. Kuo et al.

[Title Page](#)

[Abstract](#)

[Introduction](#)

[Conclusions](#)

[References](#)

[Tables](#)

[Figures](#)

[◀](#)

[▶](#)

[◀](#)

[▶](#)

[Back](#)

[Close](#)

[Full Screen / Esc](#)

[Printer-friendly Version](#)

[Interactive Discussion](#)



4 Effect of stem flow on energy flux

The results in last section show that stem–root flow can alter the vertical profile of soil moisture. It is important to know whether such a modification has significant effects on evapotranspiration and associated interactions between the land and atmosphere.

5 The soil moisture in the top soil layer in the LHC case generally decreased due to stem–root flow, except in some instances (e.g., mid-September, the later dry season) when the enhanced moisture storage in the deep layers replenish the moisture in the drying surface soil through moisture diffusion. The drying of the surface soil resulted in less soil evaporation (Fig. 6a) and thus weaker latent heat release (see Table 4 for the mean and maximum changes in daily temperatures and energy fluxes). This led to a higher soil surface temperature and consequently stronger sensible heat flux (blue curve in Fig. 6b), which resulted in warmer air (magenta curve in Fig. 7b) and thus stronger rainwater evaporation from the leaf surface (green curve in Fig. 6a). However, changes in plant transpiration were insignificant (red curve in Fig. 6a), as this process is associated with soil moisture not only in the top layer but also in the deeper layers that are within the reach of the root system. Therefore, the effect of surface layer drying on transpiration may be compensated by the moistening of the lower layers. Furthermore, in the LHC case, the moisture of all soil layers was maintained well above the wilting point, and normal transpiration could be maintained throughout the year. The decrease in latent heat therefore resulted mainly from changes in soil evaporation in the LHC case.

15 In the HAPEX case, the stem–root flow caused a general drying of the top soil, except for a brief period in mid-October (Fig. 7a). However, responses in soil evaporation were not as straightforward as in the LHC case. For example, in late July (just after the start of the growing season) there was a spike in the evaporation but a reduction in the moisture of the top soil layer (blue curve in Fig. 7a). As wind speed is the same for both cases, the increase in soil evaporation must be due to either a higher soil temperature and/or a lower water vapor density in the air near the soil surface. This was indeed

Stem-root flow effect on soil–atmosphere interactions and uncertainty assessments

T.-H. Kuo et al.

Title Page

Abstract

Introduction

Conclusions

References

Tables

Figures

⏪

⏩

◀

▶

Back

Close

Full Screen / Esc

Printer-friendly Version

Interactive Discussion



Stem-root flow effect on soil–atmosphere interactions and uncertainty assessments

T.-H. Kuo et al.

[Title Page](#)

[Abstract](#)

[Introduction](#)

[Conclusions](#)

[References](#)

[Tables](#)

[Figures](#)

[⏪](#)

[⏩](#)

[◀](#)

[▶](#)

[Back](#)

[Close](#)

[Full Screen / Esc](#)

[Printer-friendly Version](#)

[Interactive Discussion](#)

Even with the maximum V_s , the simulated soil moistures at the bottom layer are still lower than observed. More realistic values for other soil physical parameters and/or optimizations of these parameters are required. Xue et al. (1996) pointed out that land surface models such as SSiB are quite sensitive to soil-type dependent parameters such as the hydraulic conductivity at saturation and the coefficient used to calculate soil water potential. Such parameters can vary significantly from place to place, and sufficient information to assign appropriate values is usually lacking. This is particularly true for LHC where the soil types exhibited a rather inhomogeneous vertical distribution, and some humus layers could exist to retard surface drainage. Another critical issue is the treatment of water flow across the bottom soil layer. In our current model, soil water can leave the bottom layer with a fixed efficiency, but no recharge from the water table below is allowed. These issues might cause the model to underestimate the soil moisture in the bottom layer (regardless of the presence of stem–root flow), which occurred in both the LHC and HAPEX simulations (cf. Figs. 4c and 5c).

Henderson-Sellers (1996) indicated that a full evaluation of land surface model's simulation against observations can be established only when the initial conditions and all soil parameters are known precisely. Since this exploratory study focuses on introducing the stem–root flow mechanisms in a land surface model and test its possible impact, we will not further test the uncertainty due to other parameters in this paper. We hope more relevant measurements will provide useful information to study these issues further.

6 Conclusion

In this study, a stem–root flow mechanism, which provides an efficient water channel for rain to penetrate into deep soil, was formulated and implemented into an offline version of the SSiB land–atmosphere model. The model was used to simulate soil moisture variation at two sites with different climate and ecology conditions: LHC with a mountain rainforest climate and HAPEX with a Mediterranean climate. The results showed that

**Stem-root flow effect
on soil–atmosphere
interactions and
uncertainty
assessments**

T.-H. Kuo et al.

[Title Page](#)[Abstract](#)[Introduction](#)[Conclusions](#)[References](#)[Tables](#)[Figures](#)[⏪](#)[⏩](#)[◀](#)[▶](#)[Back](#)[Close](#)[Full Screen / Esc](#)[Printer-friendly Version](#)[Interactive Discussion](#)

the inclusion of the stem–root flow mechanism substantially improved the capability of the model to simulate vertical soil moisture profiles. Stem–root flow generally caused a drying of the top soil layer (upper 20 cm) and a moistening of the bottom layer (below 50 cm) in the model. On a few occasions, such as after a long dry period, the surface layer may be less dry than without the stem–root flow due to greater water supply from the lower layers. The middle soil layer at LHC was also moistened and, in many instances during rainfall events, the moisture in this layer fluctuated more intensely than in the top layer in response to the stem–root flow. However, in the HAPEX case, the middle layer became dryer with less fluctuation. Due to differences in plant and soil types, the strength of the stem–root flow was greater at LHC than at HAPEX.

The change in soil moisture associated with the stem–root flow leads to significant modifications in heat and moisture fluxes between the land and atmosphere. The general drying of the surface soil leads to reduced soil evaporation and thus increased soil temperature. Plant transpiration at LHC was not significantly affected by the stem flow because the soil moisture content was maintained well above the wilting point. Therefore, the stem–root flow related to energy flux between the soil and atmosphere is mainly controlled by sensible heat. In this sense, LHC may be considered as having an energy-limited evapotranspiration regime. In contrast, the HAPEX soil (especially the top layer) was generally dryer and sometimes fell below the wilting point. Plant transpiration can thus be substantially affected by the stem–root flow. Changes in transpiration lead to changes in air temperature, which, in turn, influence soil temperature. This effect is stronger than that resulting from the soil evaporation associated with changes in the soil moisture of the top soil layer. At the HAPEX site, evapotranspiration was more soil moisture-limited than energy-limited, and its net change in heat flux associated with the stem–root flow was dominated by latent heat. While the stem–root flow effect on soil moisture was weaker there than at LHC, the energy flux exchanges were actually stronger due to the sensitive transpiration process.

Through the impact on soil moisture profiles, stem–root flow can significantly affect evaporation and transpiration processes. The associated changes in moisture and en-

Stem-root flow effect on soil–atmosphere interactions and uncertainty assessments

T.-H. Kuo et al.

[Title Page](#)

[Abstract](#)

[Introduction](#)

[Conclusions](#)

[References](#)

[Tables](#)

[Figures](#)

[⏪](#)

[⏩](#)

[◀](#)

[▶](#)

[Back](#)

[Close](#)

[Full Screen / Esc](#)

[Printer-friendly Version](#)

[Interactive Discussion](#)



ergy fluxes between the land and atmosphere may affect boundary-layer stability and convective processes. As evapotranspiration returns as much as 60 % of the precipitation back to the atmosphere over land (Oki and Kanae, 2006), the stem–root flow mechanism may be a key factor in controlling the surface water budget and hydrological cycle. The enhanced storage of water in deep soil layers may have a long-term effect on the climate system. These issues are worthy of further investigation through more relevant observations and testing by coupling the stem–root flow mechanism with global climate models.

Appendix: Derivation of D_{eff}

The parameter D_{eff} in Eq. (4) was derived in a similar fashion as in Zimmerman and Bodvarsson (1991). The soil water horizontal (x direction) movement can be express as following:

$$\rho \frac{\partial \theta}{\partial t} = \frac{\partial}{\partial x} \left[K(\Psi) \frac{\partial \Psi}{\partial x} \right] \quad (\text{A1})$$

where ρ is soil porosity; θ is the ratio of soil water content to its saturated state; K (in m s^{-1}) is the hydraulic conductivity of the soil; and Ψ (in m) is the soil water potential. Equation (A1) is subject to the following initial and boundary conditions:

$$\theta(0, t) = 1, \quad \theta(x, 0) = \theta_w, \quad \theta(x \rightarrow \infty, t) = \theta_w. \quad (\text{A2})$$

The first condition means that, when the root-flow occurs, soil at the root–soil interface ($x = 0$) is saturated. The next two conditions specify the initial bulk soil water content, θ_w , and this value remains unaffected by the root flow at a far distance from the root–soil interface throughout the integration time period.

The hydraulic conductivity and water potential of the soil can be represented with the empirical relationship of Clapp and Hornberger (1978):

$$K(\Psi) = K_s \left(\Psi / \Psi_s \right)^{-\frac{3}{b} + 2} \quad (\text{A3})$$

$$\Psi = -\Psi_s \theta^b, \quad (\text{A4})$$

where K_s (in ms^{-1}) is hydraulic conductivity at saturation; b is an empirical constant dependent on the soil type. By introducing a similarity variable η and two normalized variables $\hat{\Psi}$ and \hat{K} :

$$\eta \equiv \sqrt{\frac{\rho}{K_s \Psi_s t}}, \quad \hat{\Psi} \equiv \frac{\Psi}{\Psi_s}, \quad \text{and} \quad \hat{K} \equiv \frac{K}{K_s}, \quad (\text{A5})$$

Eq. (A1) can be transformed into

$$\frac{d}{d\eta} \left(\hat{K}(\hat{\Psi}) \frac{d\hat{\Psi}}{d\eta} \right) + \frac{\eta}{2} \frac{d\theta}{d\eta} = 0, \quad (\text{A6})$$

whereas the initial and boundary conditions in Eq. (A2) reduced to

$$\theta(0) = 1, \quad \theta(\eta \rightarrow \infty) = \theta_w \quad (\text{A7})$$

Zimmerman and Bodvarsson (1991) showed that the solution for Eq. (A6) with conditions in Eq. (A7) can be approximated as:

$$\begin{cases} \theta = 1 & , \text{ if } 0 \leq \eta \leq \lambda \\ \theta = 1 - (1 - \theta_w) \frac{\eta - \lambda}{\delta} & , \text{ if } \lambda < \eta \leq \lambda + \delta \\ \theta = \theta_w & , \text{ if } \lambda + \delta < \eta < \infty \end{cases} \quad (\text{A8})$$

where

$$\delta = 2 \sqrt{\frac{b}{1 + \frac{2}{b(1 - \theta_w)}}} \quad \text{and} \quad \lambda = \frac{\delta}{b(1 - \theta_w)} \quad (\text{A9})$$

Stem-root flow effect on soil–atmosphere interactions and uncertainty assessments

T.-H. Kuo et al.

[Title Page](#)

[Abstract](#)

[Introduction](#)

[Conclusions](#)

[References](#)

[Tables](#)

[Figures](#)

[⏪](#)

[⏩](#)

[◀](#)

[▶](#)

[Back](#)

[Close](#)

[Full Screen / Esc](#)

[Printer-friendly Version](#)

[Interactive Discussion](#)



That is, within the root–soil boundary ($0 \leq \eta \leq \lambda$), θ is saturated ($= 1$); whereas in the transition zone ($\lambda < \eta \leq \lambda + \delta$), θ decreases linearly from 1 to θ_w . Here, δ is the “effective thickness” of diffusion in the η coordinate, and it can be revert back to the x coordinate using the similarity conversion in Eq. (A5):

$$D_{\text{eff}} = \delta \sqrt{\frac{K_s \Psi_s t}{\rho}} \quad (\text{A10})$$

By applying the actual rainfall duration for t into Eq. (A10), we calculated the mean values of $D_{\text{eff}} = 0.005$ m for the HAPEX site and $D_{\text{eff}} = 0.03$ m for the LHC site.

Acknowledgement. This study was supported by the Ministry of Science and Technology of the Republic of China on Taiwan through project NSC–100–2119–M–002–023–MY5. Y. Xue’s support is from US NSF AGS-1346813. We are also grateful to S. Sun for technical assistance on SSiB, M.-H. Li and Y.-Y. Chen for providing observation data, and W.-L. Liang for helpful suggestions.

References

- André, F., Jonard, M., and Ponette, Q.: Influence of species and rain event characteristics on stemflow volume in a temperate mixed oak–beech stand, *Hydrol. Process.*, 22, 4455–4466, doi:10.1002/hyp.7048, 2008.
- Bohm, W.: *Methods of Studying Root Systems*, Ecological Studies Volume 33, Springer, Berlin, Heidelberg, New York, 1979.
- Beven, K. and Germann, P.: Macropores and water flow in soils, *Water Resour. Res.*, 18, 1311–1325, doi:10.1029/WR018i005p01311, 1982.
- Budyko, M. I.: *Climate and Life*, Academic Press, New York, 1974.
- Chase, T. N., Pielke, R. A., Kittel, T. G. F., Nemani, R., and Running, S. W.: Sensitivity of a general circulation model to global changes in leaf area index, *J. Geophys. Res.-Atmos.*, 101, 7393–7408, doi:10.1029/95jd02417, 1996.
- Chase, T. N., Pielke Sr., R. A., Kittel, T. G. F., Nemani, R. R., and Running, S. W.: Simulated impacts of historical land cover changes on global climate in northern winter, *Clim. Dynam.*, 16, 93–105, doi:10.1007/s003820050007, 2000.

Stem-root flow effect on soil–atmosphere interactions and uncertainty assessments

T.-H. Kuo et al.

[Title Page](#)

[Abstract](#)

[Introduction](#)

[Conclusions](#)

[References](#)

[Tables](#)

[Figures](#)

[⏪](#)

[⏩](#)

[◀](#)

[▶](#)

[Back](#)

[Close](#)

[Full Screen / Esc](#)

[Printer-friendly Version](#)

[Interactive Discussion](#)



**Stem-root flow effect
on soil–atmosphere
interactions and
uncertainty
assessments**

T.-H. Kuo et al.

[Title Page](#)[Abstract](#)[Introduction](#)[Conclusions](#)[References](#)[Tables](#)[Figures](#)[⏪](#)[⏩](#)[◀](#)[▶](#)[Back](#)[Close](#)[Full Screen / Esc](#)[Printer-friendly Version](#)[Interactive Discussion](#)

Chen, Y.-Y.: Investigating the Seasonal Variability of Surface Heat and Water Vapor Fluxes with Eddy Covariance Techniques: a Subtropical Evergreen Forest as an Example, Doctoral, Graduate Institute of Hydrological and Oceanic Sciences, National Central University, Taoyuan City, Taiwan, 149 pp., 2012.

5 Clapp, R. B. and Homberger, G. M.: Empirical equations for some soil hydraulic properties, *Water Resour. Res.*, 14, 601–604, 1978.

Dorman, J. L. and Sellers, P. J.: A. Global climatology of albedo, roughness length and stomatal resistance for atmospheric general circulation models as represented by the Simple Biosphere Model (SiB), *J. Appl. Meteorol.*, 28, 833–855, doi:10.1175/1520-0450(1989)028<0833:agcoar>2.0.co;2, 1989.

10 Gerke, H.: Bypass flow in soil, in: *Encyclopedia of Agrophysics*, edited by: Gliński, J., Horabik, J., and Lipiec, J., *Encyclopedia of Earth Sciences Series*, Springer, the Netherlands, 100–105, 2014.

Goutorbe, J. P.: A Critical assessment of the Samer network accuracy, in: *Land Surface Evaporation*, edited by: Schmugge, T., and André, J.-C., Springer New York, 171–182, 1991.

15 Goutorbe, J. P. and Tarrieu, C.: HAPEX-MOBILHY data base, in: *Land Surface Evaporation*, edited by: Schmugge, T., and André, J.-C., Springer, New York, 403–410, 1991.

Goutorbe, J.-P., J. Noilhan, C. Valancogne, and Cuenca, R. H.: Soil moisture variations during HAPEX-MOBILHY, *Ann. Geophys.-Italy*, 7, 415–426, 1989.

20 Henderson-Sellers, A.: Soil moisture simulation: achievements of the RICE and PILPS inter-comparison workshop and future directions. *Global Planet. Chang.*, 13, Issues 1–4, 99–115, doi:10.1016/0921-8181(95)00035-6, 1996

Jarvis, N. J. and Dubus, I. G.: State-of-the-art review on preferential flow, Report DL#6 of the FP6 EU-funded FOOTPRINT Project, available at: <http://www.eu-footprint.org> (last access: 5 June 2012), 60 pp., 2006.

25 Johnson, M. S. and Lehmann, J.: Double-funneling of trees: stemflow and root-induced preferential flow, *Ecoscience*, 13, 324–333, 2006.

Köhne, J. M., Köhne, S., and Šimůnek, J.: A review of model applications for structured soils: a) Water flow and tracer transport, *J. Contam. Hydrol.*, 104, 4–35, doi:10.1016/j.jconhyd.2008.10.002, 2009.

30 Levia, D. F. and Frost, E. E.: A review and evaluation of stemflow literature in the hydrological and biochemical cycles of forested and agricultural ecosystems., *J. Hydrol.*, 274, 1–29, 2003.

Stem-root flow effect on soil–atmosphere interactions and uncertainty assessments

T.-H. Kuo et al.

[Title Page](#)

[Abstract](#)

[Introduction](#)

[Conclusions](#)

[References](#)

[Tables](#)

[Figures](#)

[⏪](#)

[⏩](#)

[◀](#)

[▶](#)

[Back](#)

[Close](#)

[Full Screen / Esc](#)

[Printer-friendly Version](#)

[Interactive Discussion](#)

- Li, J., He, B., Chen, Y., Huang, R., Tao, J., and Tian, T.: Root distribution features of typical herb plants for slope protection and their effects on soil shear strength, *Transactions of the Chinese Society of Agricultural Engineering*, 29, 144–152, 2013.
- Xiao-Yan Li, Zhi-Peng Yang, Yue-Tan Li, and Henry Lin: Connecting ecohydrology and hydrope-
 5 dology in desert shrubs: stemflow as a source of preferential flow in soils, *Hydrol. Earth Syst. Sci.*, 13, 1133–1144, doi:10.5194/hess-13-1133-2009, 2009.
- Li, X.-Y., Lin, H., and Levia, D. F.: Coupling ecohydrology and hydrogeology at different spatio-temporal scales in water-limited ecosystems, in: *Hydrogeology*, edited by: Lin, H., Academic Press, Boston, 737–758, 2012.
- 10 Liang, W.-L., Kosugi, K. i., and Mizuyama, T.: Heterogeneous soil water dynamics around a tree growing on a steep hillslope, *Vadose Zone J.*, 6, 879–889, doi:10.2136/vzj2007.0029, 2007.
- Liu, I.-W. Y., Waldron, L. J., and Wong, S. T. S.: Application of nuclear magnetic resonance imaging to study preferential water flow through root channels, *SSSA Spec. Publ.*, 36, Tomography of Soil-Water-Root Processesm 135–148, doi:10.2136/sssaspecpub36.c11,
 15 1994.
- McGuffie, K., Henderson-Sellers, A., Zhang, H., Durbidge, T. B., and Pitman, A. J.: Global climate sensitivity to tropical deforestation, *Global Planet. Change*, 10, 97–128, doi:10.1016/0921-8181(94)00022-6, 1995.
- Návar, J.: The causes of stemflow variation in three semi-arid growing species of northeastern
 20 Mexico, *J. Hydrol.*, 145, 175–190, doi:10.1016/0022-1694(93)90226-Y, 1993.
- Neave, M. and Abrahams, A. D.: Vegetation influences on water yields from grassland and shrubland ecosystems in the Chihuahuan Desert, *Earth Surf. Proc. Land.*, 27, 1011–1020, doi:10.1002/esp.389, 2002.
- Oki, T. and Kanae, S.: Global Hydrological Cycles and World Water Resources. *Science*, 313,
 25 1068–1072, 2006.
- Sellers, P. J., Mintz, Y., Sud, Y. C., and Dalcher, A.: A Simple Biosphere Model (SIB) for use within general circulation models, *J. Atmos. Sci.*, 43, 505–531, doi:10.1175/1520-0469(1986)043<0505:ASBMFU>2.0.CO;2, 1986.
- Seneviratne, S. I., Corti, T., Davin, E. L., Hirschi, M., Jaeger, E. B., Lehner, I., Orlowsky, B., and Teuling, A. J.: Investigating soil moisture–climate interactions in a changing climate: a review,
 30 *Earth-Sci. Rev.*, 99, 125–161, doi:10.1016/j.earscirev.2010.02.004, 2010.

**Stem-root flow effect
on soil–atmosphere
interactions and
uncertainty
assessments**

T.-H. Kuo et al.

[Title Page](#)[Abstract](#)[Introduction](#)[Conclusions](#)[References](#)[Tables](#)[Figures](#)[⏪](#)[⏩](#)[◀](#)[▶](#)[Back](#)[Close](#)[Full Screen / Esc](#)[Printer-friendly Version](#)[Interactive Discussion](#)

Siegert, C. M. and Levina, D. F.: Seasonal and meteorological effects on differential stemflow funneling ratios for two deciduous tree species, *J. Hydrol.*, 519, 446–454, doi:10.1016/j.jhydrol.2014.07.038, 2014.

Tanaka, T., Taniguchi, M., and Tsujimura, M.: Significance of stemflow in groundwater recharge. 2: A cylindrical infiltration model for evaluating the stemflow contribution to groundwater recharge, *Hydrol. Process.*, 10, 81–88, doi:10.1002/(sici)1099-1085(199601)10:1<81::aid-hyp302>3.0.co;2-m, 1996.

Taniguchi, M., Tsujimura, M., and Tanaka, T.: Significance of stemflow in groundwater recharge. 1: Evaluation of the stemflow contribution to recharge using a mass balance approach, *Hydrol. Process.*, 10, 71–80, doi:10.1002/(sici)1099-1085(199601)10:1<71::aid-hyp301>3.0.co;2-q, 1996.

Wu, B.-Y.: Simulations of Land Surface Fluxes of the Lien Hua Chih Experimental Watershed with Land Process Models, Master, Graduate Institute of Hydrological and Oceanic Sciences, National Central University, Taoyuan City, Taiwan, 100 pp., 2011.

Xue, Y., Sellers, P., Kinter, J., and Shukla, J.: A simplified biosphere model for global climate studies, *J. Climate*, 4, 345–364, 1991.

Xue, Y., Zeng, F. J., and Adam Schlosser, C.: SSiB and its sensitivity to soil properties – a case study using HAPEX-Mobilhy data, *Global Planet. Change*, 13, 183–194, doi:10.1016/0921-8181(95)00045-3, 1996.

Zhang, Y.-Q., Zhu, Q. K., and Qi, S.: Root system distribution characteristics of plants on the terrace banks and their impact on soil moisture, *Acta Ecol. Sin.*, 25, 500–506, 2005.

Zhao, M., Pitman, A. J., and Chase, T.: The impact of land cover change on the atmospheric circulation, *Clim. Dynam.*, 17, 467–477, doi:10.1007/pl00013740, 2001.

Zimmerman, R. and Bodvarsson, G.: A simple approximate solution for horizontal infiltration in a Brooks-Corey medium. *Transport Porous Med.*, 6, 195–205, 1991.

Stem-root flow effect on soil–atmosphere interactions and uncertainty assessments

T.-H. Kuo et al.

Table 1. Basic parameters used for describing the LHC and HAPEX sites. LHC data were obtained from Wu (2011); HAPEX data were obtained from Goutorbe et al. (1989).

Location	LHC	HAPEX
Annual rainfall	2316 mm	856 mm
Mean temperature	19.7 °C	8.6 °C
Altitude	770 m	113 m
Vegetation cover	Rainforest of mixed evergreens and hardwoods	Soya crop
Soil type	Loam	17 % clay content, 46 % silt, 37 % sand
Soil moisture measurement depth	10, 30, 50, 70, 90 cm	Every 10 cm down to 160 cm
Soil wetness exponent	2.5	5.66
Soil tension at saturation	−0.1	−0.30
Hydraulic conductivity at saturation	1×10^{-6}	4×10^{-6}
Soil porosity	0.530	0.446
Slope	0.55	0.05

Title Page

Abstract

Introduction

Conclusions

References

Tables

Figures

◀

▶

◀

▶

Back

Close

Full Screen / Esc

Printer-friendly Version

Interactive Discussion

HESSD

12, 11783–11816, 2015

Stem-root flow effect on soil–atmosphere interactions and uncertainty assessments

T.-H. Kuo et al.

Table 2. Monthly leaf area index values for LHC in 2010 and HAPEX in 1986. LHC data were obtained from Wu (2011); HAPEX data were obtained from Goutorbe et al. (1989)

Month	1	2	3	4	5	6	7	8	9	10	11	12
LHC	3.34	3.08	3.06	3.04	4.35	4.77	4.84	4.91	4.66	4.4	4.2	4.25
HAPEX	0	0	0	0	1	3	3	3	3	0	0	0

[Title Page](#)[Abstract](#)[Introduction](#)[Conclusions](#)[References](#)[Tables](#)[Figures](#)[⏪](#)[⏩](#)[◀](#)[▶](#)[Back](#)[Close](#)[Full Screen / Esc](#)[Printer-friendly Version](#)[Interactive Discussion](#)

Stem-root flow effect on soil–atmosphere interactions and uncertainty assessments

T.-H. Kuo et al.

Table 3. The mean bias, root-mean-square error (RMSE), and standard deviation (STD) in simulated soil moisture comparing to observations (obs). “Control” stands for simulations without the stem–root flow mechanism, and “SLR90 %” or “SLR50 %” are simulations with the optimal stemflow to leaf drainage ratio.

	SM1			SM2			SM3		
	bias	RMSE	STD	bias	RMSE	STD	bias	RMSE	STD
LHC control-obs	−0.003	0.142	0.142	−0.098	0.153	0.012	−0.141	0.193	0.131
LHC SLR90 %-obs	0.023	0.056	0.051	−0.034	0.050	0.036	−0.038	0.048	0.029
HAPEX control-obs	0.018	0.036	0.032	0.032	0.037	0.019	−0.057	0.085	0.063
HAPEX SLR50 %-obs	0.009	0.030	0.029	0.024	0.030	0.018	−0.049	0.074	0.056

[Title Page](#)
[Abstract](#)
[Introduction](#)
[Conclusions](#)
[References](#)
[Tables](#)
[Figures](#)
[Back](#)
[Close](#)
[Full Screen / Esc](#)
[Printer-friendly Version](#)
[Interactive Discussion](#)

Stem-root flow effect on soil–atmosphere interactions and uncertainty assessments

T.-H. Kuo et al.

Table 4. Mean and maximum changes in daily temperatures and energy fluxes due to the stem–root flow (between optimal SLR run and control run) during the growing season. Canopy air temperature (T_C), soil surface temperature (T_S) and leaf temperature (T_L) are in $^{\circ}\text{C}$; Transpiration (TR), soil evaporation (SE), leaf evaporation (LE), sensible heat (SH) and latent heat (LH) are in Wm^{-2} .

	ΔT_C	ΔT_S	ΔT_L	ΔTR	ΔSE	ΔLE	ΔSH	ΔLH
LHC mean	0.32	0.31	0.34	0.20	−1.19	0.31	2.02	−0.68
LHC maximum	2.90	2.59	3.18	1.01	−15.50	11.34	31.44	−16.81
HAPEX mean	0.04	0.11	0.03	1.06	−2.17	0.28	0.52	−0.82
HAPEX maximum	1.27	1.63	1.70	−66.74	−19.5	9.95	51.16	−66.29

Title Page

Abstract

Introduction

Conclusions

References

Tables

Figures

◀

▶

◀

▶

Back

Close

Full Screen / Esc

Printer-friendly Version

Interactive Discussion

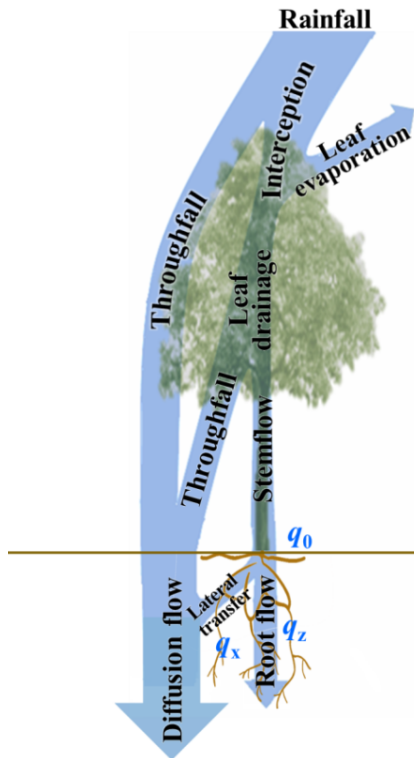


Figure 1. Stem-root flow conceptual diagram. Leaf drainage in the model can be separated into throughfall and stemflow. Following the stemflow path, rainwater can continue via the root system to reach deep soil layers and the water table. The stemflow that reaches the soil top, q_0 , is divided into a downward transfer flux (i.e., the root flow) q_z and a lateral transfer flux q_x (from the root surface to the soil), and the two transfer fluxes regulate the root flow thickness.

Stem-root flow effect on soil–atmosphere interactions and uncertainty assessments

T.-H. Kuo et al.

Title Page

Abstract Introduction

Conclusions References

Tables Figures

◀ ▶

◀ ▶

Back Close

Full Screen / Esc

Printer-friendly Version

Interactive Discussion



**Stem-root flow effect
on soil–atmosphere
interactions and
uncertainty
assessments**

T.-H. Kuo et al.

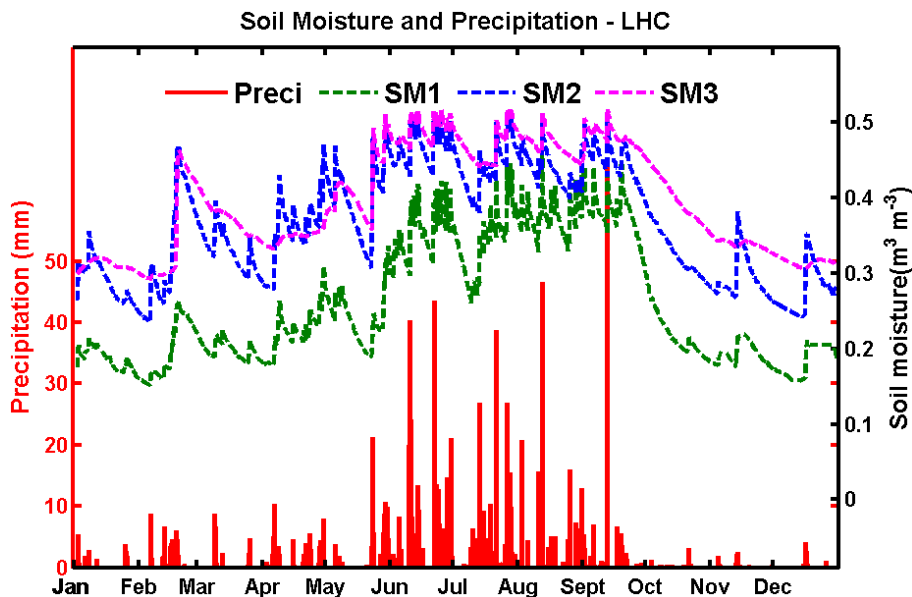


Figure 2. The hourly soil moisture (curves, right axis) and precipitation (red bars, left axis) observed at LHC during 2010. SM1, SM2 and SM3 represent soil moisture at 10 cm (green-dashed curve), 40 cm (blue-dashed curve; average of 30 and 50 cm observations) and 90 cm (magenta-dashed curve), respectively.

[Title Page](#)[Abstract](#)[Introduction](#)[Conclusions](#)[References](#)[Tables](#)[Figures](#)[◀](#)[▶](#)[◀](#)[▶](#)[Back](#)[Close](#)[Full Screen / Esc](#)[Printer-friendly Version](#)[Interactive Discussion](#)

Stem-root flow effect on soil–atmosphere interactions and uncertainty assessments

T.-H. Kuo et al.

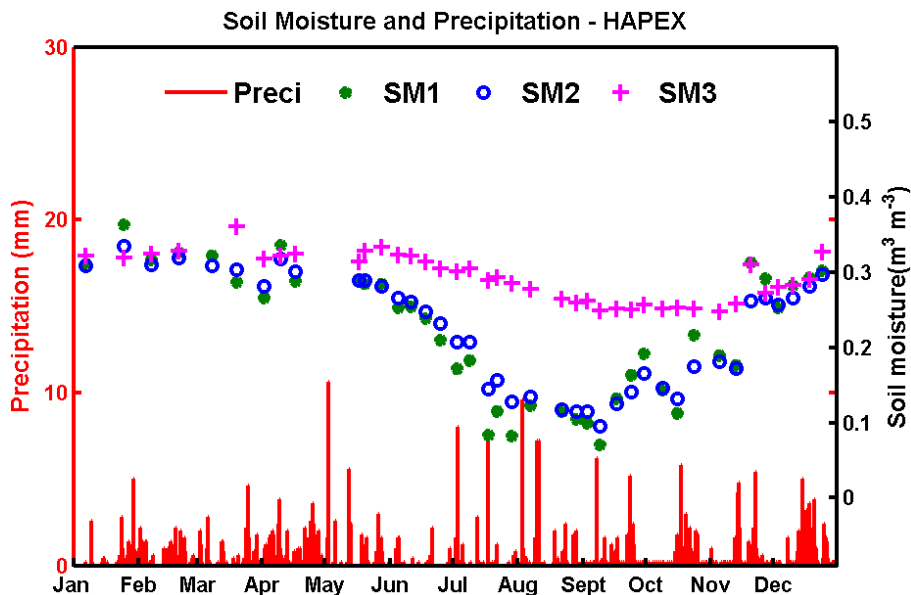


Figure 3. The weekly soil moisture (symbols, right axis) and hourly precipitation (red bars, left axis) observed at HAPEX during 1986. SM1 SM2 and SM3 represent the mean soil moisture in the 0–20 cm (green dot), 20–50 cm (blue circle), and 50–160 cm (magenta cross) layers, respectively.

[Title Page](#)

[Abstract](#)

[Introduction](#)

[Conclusions](#)

[References](#)

[Tables](#)

[Figures](#)

[◀](#)

[▶](#)

[◀](#)

[▶](#)

[Back](#)

[Close](#)

[Full Screen / Esc](#)

[Printer-friendly Version](#)

[Interactive Discussion](#)

Stem-root flow effect on soil–atmosphere interactions and uncertainty assessments

T.-H. Kuo et al.

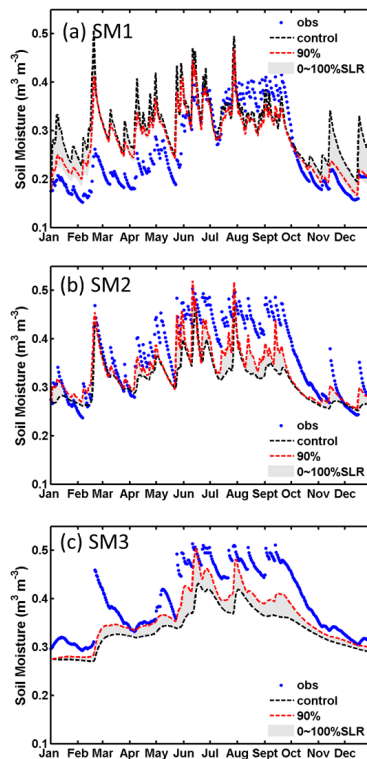


Figure 4. Simulated and observed soil moisture for the LHC site at depths of **(a)** SM1 (0–20 cm), **(b)** SM2 (20–70 cm), and **(c)** SM3 (70–170 cm). Observed results are shown as blue dots. Simulations with SLR = 0 (i.e., control run, without stem–root flow) and SLR = 90 % are shown as black-dashed and red-dashed curves, respectively. The area of grey shading enclosed by SLR = 0 % and 100 % indicates the possible range of the stem–root flow effects. All simulation results are daily averages.

[Title Page](#)
[Abstract](#)
[Introduction](#)
[Conclusions](#)
[References](#)
[Tables](#)
[Figures](#)
[⏪](#)
[⏩](#)
[◀](#)
[▶](#)
[Back](#)
[Close](#)
[Full Screen / Esc](#)
[Printer-friendly Version](#)
[Interactive Discussion](#)

Stem-root flow effect on soil–atmosphere interactions and uncertainty assessments

T.-H. Kuo et al.

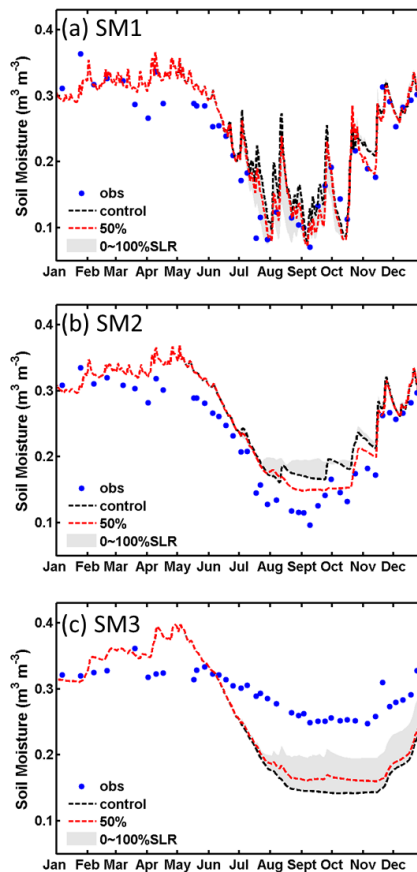


Figure 5. Same as Fig. 4, but for the HAPEX case at depths of **(a)** SM1 (0–20 cm), **(b)** SM2 (20–50 cm), and **(c)** SM3 (50–160 cm). Red-dashed curves are results with SLR = 50 %.

Stem–root flow effect on soil–atmosphere interactions and uncertainty assessments

T.-H. Kuo et al.

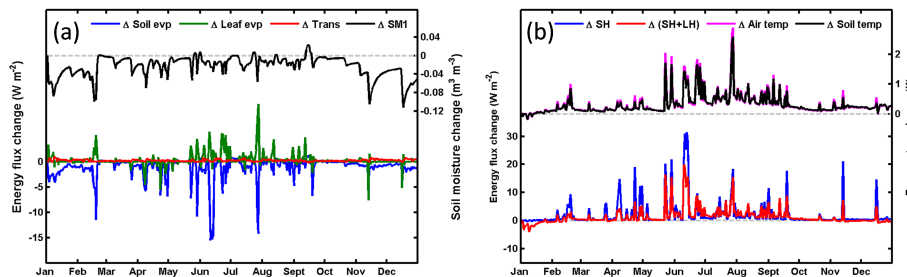


Figure 6. Difference in daily mean heat fluxes and soil moisture due to stem–root flow at the LHC case. **(a)** Changes in soil evaporation (blue curve), leaf evaporation (green curve), transpiration (red curve) and soil moisture of the surface layer (black curve; right axis); **(b)** Changes in sensible heat (blue curve), total heat (sensible heat plus latent heat; red curve), air temperature near the soil surface (magenta curve; right axis) and soil temperature (black curve; right axis). Grey dashed lines indicate the zero baseline.

[Title Page](#)

[Abstract](#)

[Introduction](#)

[Conclusions](#)

[References](#)

[Tables](#)

[Figures](#)

◀

▶

◀

▶

[Back](#)

[Close](#)

[Full Screen / Esc](#)

[Printer-friendly Version](#)

[Interactive Discussion](#)

Stem-root flow effect on soil–atmosphere interactions and uncertainty assessments

T.-H. Kuo et al.

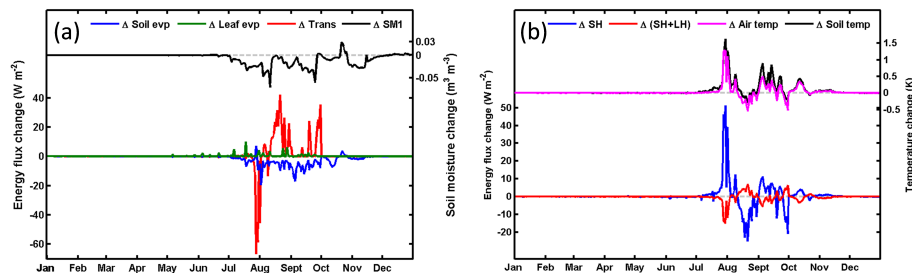


Figure 7. Same as Fig. 6, but for the HAPEX case.

Title Page

Abstract

Introduction

Conclusions

References

Tables

Figures

◀

▶

◀

▶

Back

Close

Full Screen / Esc

Printer-friendly Version

Interactive Discussion

Stem-root flow effect on soil–atmosphere interactions and uncertainty assessments

T.-H. Kuo et al.

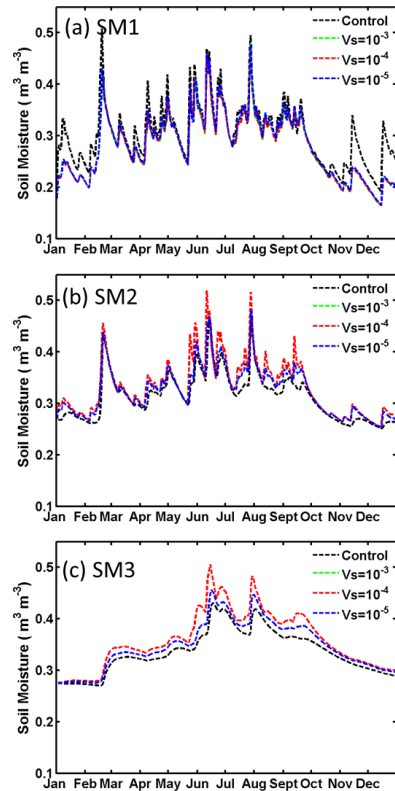


Figure 8. Sensitivity test on V_s for the LHC case with optimal SLR = 90% at depths of **(a)** SM1 (0–20 cm), **(b)** SM2 (20–70 cm), and **(c)** SM3 (70–170 cm). The green-dashed, red-dashed and blue-dashed curves are for $V_s = 10^{-3}$, 10^{-4} , and 10^{-5} m s⁻¹, respectively. Also shown in black-dashed curves are the control run results (i.e., SLR = 0).

Stem-root flow effect on soil–atmosphere interactions and uncertainty assessments

T.-H. Kuo et al.

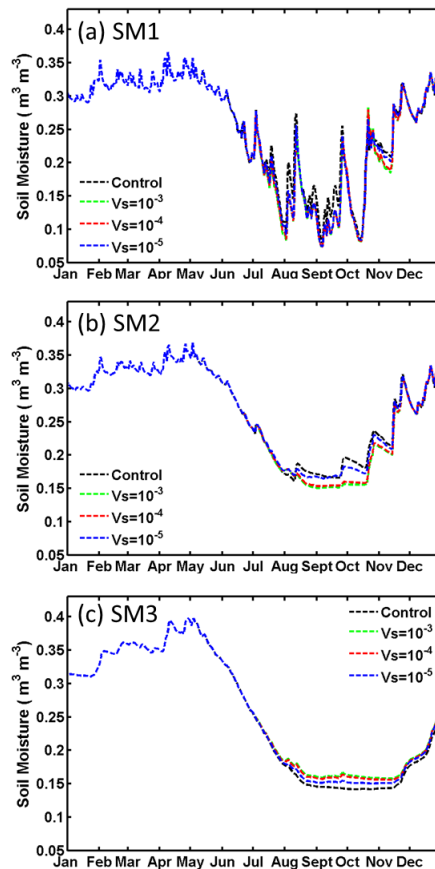


Figure 9. Same as Fig. 8, but SLR = 50 % for the HAPEX case at depths of **(a)** SM1 (0–20 cm), **(b)** SM2 (20–50 cm), and **(c)** SM3 (50–160 cm).

[Title Page](#)
[Abstract](#)
[Introduction](#)
[Conclusions](#)
[References](#)
[Tables](#)
[Figures](#)
[◀](#)
[▶](#)
[◀](#)
[▶](#)
[Back](#)
[Close](#)
[Full Screen / Esc](#)
[Printer-friendly Version](#)
[Interactive Discussion](#)